Published by Associazione Teriologica Italiana
Hystrix, the Italian Journal of Mammalogy
Volume 24 (1): 103–109, 2013
Available online at:
http://www.italian-journal-of-mammalogy.it/article/view/6292/pdf
doi:10.4404/hystrix-24.1-6292

Research Article

Semilandmarks: a method for quantifying curves and surfaces

Philipp Gunz[a,*], Philipp Mitteroecker[b]

[a] *Department of Human Evolution, Max Planck Institute for Evolutionary Anthropology, Leipzig, Germany*
[b] *Department of Theoretical Biology, University of Vienna, Vienna, Austria*

Keywords:
Procrustes
geometric morphometrics
virtual reconstruction

Article history:
Received: 31 May 2012
Accepted: 29 July 2012

Acknowledgements
We want to thank Andrea Cardini for the invitation to contribute to this issue. The data in Figs. 4 and 5 were collected by Sarah Freidline. We thank Peter Brugger for access to the human brain MRI scans used in Fig. 2 and 3. Comments and suggestions by two expert referees helped improve the manuscript.

Abstract

Quantitative shape analysis using geometric morphometrics is based on the statistical analysis of landmark coordinates. Many structures, however, cannot be quantified using traditional landmarks. Semilandmarks make it possible to quantify two or three-dimensional homologous curves and surfaces, and analyse them together with traditional landmarks. Here we first introduce the concept of sliding semilandmarks and discuss applications and limitations of this method. In a second part we show how the sliding semilandmark algorithm can be used to estimate missing data in incomplete specimens.

Introduction

Here we illustrate a geometric morphometric measurement protocol, usually referred to as semilandmarks or sliding landmarks, for analysing homologous points locations together with curves and surfaces measured on a sample of organisms in two or three dimensions. Shape analysis using geometric morphometrics (GM) is based on the statistical analysis of landmark coordinates (Bookstein, 1991; Dryden and Mardia, 1998; Adams et al., 2004; Slice, 2007; Mitteroecker and Gunz, 2009). Landmarks are point locations that are biologically homologous between specimens. Many structures, however, cannot be quantified using traditional landmarks. Muscle attachments, for example, often are visible on bones, but traditional homologous landmark are insufficient to capture their shape. Smooth two- or three-dimensional curves (outlines) or surfaces, such as the neurocranial surface of a skull, are difficult to represent by landmarks because the landmark positions along the curve or surface cannot be homologized across different individuals. Semilandmarks make it possible to quantify two- or three-dimensional homologous curves and surfaces, and to analyse them together with traditional landmarks. Here we describe the concept of sliding semilandmarks and discuss possible applications and limitations of this method. We illustrate their application by several empirical examples. For a more technical discussion of semilandmarks and algebraic details see Bookstein (1997) and Gunz et al. (2005).

The concept of sliding semilandmarks was first introduced in Bookstein (1991) and published in detail for two-dimensional curves in Bookstein (1997). The method was later extended to three-dimensional curves and surfaces in Gunz et al. (2005). There are two alternative computational approaches to sliding semilandmarks, based on the two core techniques of geometric morphometrics, the Procrustes superimposition (Rohlf and Slice, 1990) and the thin-plate spline (TPS) deformation (Bookstein, 1989, 1991): Procrustes superimposition converts the raw landmark coordinates into shape coordinates by standardizing scale, position, and orientation of the landmark configurations. The Procrustes distance between two specimens (usually approximated by the Euclidean distance between the two sets of shape coordinates) is a measure of shape difference between two objects: it is zero only when two objects have the same shape. Procrustes distance also is the natural metric in Procrustes shape space (Kendall, 1984). The thin-plate spline (TPS) is an interpolation algorithm that serves as the mathematical underpinning of intuitive visualizations of shape differences, either as transformation grids or as warped images or surfaces (Fig. 1).

A TPS deformation visualizes the shape difference between one reference form and one target form, based on a set of homologous point coordinates measured on both forms. The space in-between the measured landmarks is interpolated by the TPS function "as smoothly as possible". More technically, the TPS minimizes the integral of the squared second derivatives, a quantity referred to as bending energy, which measures the amount of local shape deformation using a mathematical model borrowed from engineering (Bookstein, 1989)s. Transformation grids tell the reader how one would have to "squeeze and stretch" the reference shape to arrive at the target shape. Hand-drawn transformation grids were introduced by D'Arcy Thompson (1917); the TPS function makes it possible to produce transformation grids according to a mathematical model (for details on the mathematics see Bookstein 1989, 1991). In Fig. 1, a modern human surface is warped into a gibbon based on a large number of landmarks and semilandmarks. The TPS transformation grid visualizes the deformation from the human shape to the gibbon shape in the midsagittal plane. Note that no prior superimposition of reference and target is required for computing a TPS – the affine transformations of translation, rotation, and scaling have zero bending energy.

TPS transformation grids and TPS surface warps are the best visual aids to present shape differences between two forms as deformations (Oxnard and O'Higgins, 2009). It is important to keep in mind that the smooth TPS interpolation of the space in-between the measured landmark and semilandmark coordinates is an elegant mathematical formalism that is not intended to model a particular biological growth process, or the bending properties of organic tissues.

*Corresponding author
Email address: gunz@eva.mpg.de (Philipp Gunz)

doi:10.4404/hystrix-24.1-6292

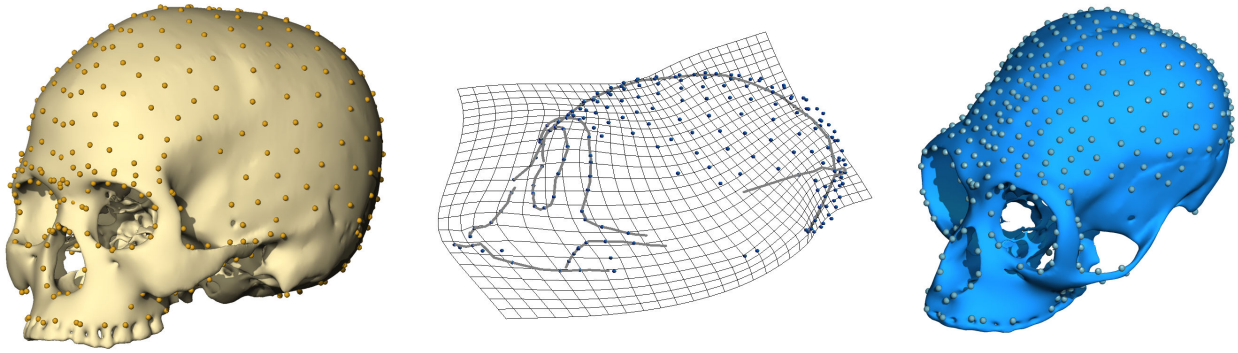

Figure 1 – Landmarks and several hundred semilandmarks measured on a computed tomographic scan of a modern human (left), and a gibbon (right). The middle panel shows the thin-plate spline (TPS) transformation grid from the human to the gibbon in the midsagittal plane. The TPS interpolation function used to draw this grid was used to warp the surface of the human cranium to the gibbon (blue surface on the right).

Point homology

In GM the measurement points are analysed with an implicit assumption about biological homology, usually based on ontogenetic or phylogenetic criteria (Bookstein, 1994; Hall, 2003; Klingenberg, 2008; Oxnard and O'Higgins, 2009). This biological homology must be expressed by a geometric homology, that is, by a point-to-point, curve-to-curve, or surface-to-surface correspondence. Furthermore, all specimens must have the same number of points. Semilandmarks are used to represent homologous curves and surfaces by sets of points, establishing a geometric homology between corresponding semilandmarks across the sample. In a first step, one distributes the same number of semilandmarks on the curves and surfaces of every specimen in roughly corresponding locations. This can either be done manually, or (semi)automatically (see below). In a second step, the spacing of the semilandmarks is optimized by allowing them to slide along the curves or surfaces (Fig. 2B). This sliding step establishes geometric correspondence of the semilandmarks by removing the effect of the arbitrary initial spacing; how the spacing is optimized differs between the two alternative computational approaches to sliding semilandmarks (Perez et al., 2006) (see below). After sliding, landmarks and semilandmarks can be treated the same way in subsequent statistical analyses. It is worth emphasizing that the rules of (semi)landmark equivalence or correspondence between forms vary according to the question at hand (Oxnard and O'Higgins 2009: 86). Oxnard and O'Higgins (2009) therefore stress that prior biological knowledge has to inform the measurement protocol, and that the choice of landmarks and semilandmarks should be driven by the biological hypotheses being tested. These authors discuss, e.g., how sagittal crests formed by the attachments of the temporal muscles in large adult male gorillas affect comparisons of neurocranial shape with female gorillas, which usually do not develop a marked crest. Below we will show that densely spaced surface semilandmarks are able to capture the shape differences between a modern human without crest, and an adult male gorilla with a marked sagittal crest (Fig. 7). In our example we treat the outer shell of the braincase in its entirety as homologous between these two specimens. While this will be helpful for many comparative purposes, inevitably this particular equivalence mapping cannot be a general solution for all possible research questions: it does not allow studying, e.g., changes in muscle attachments. Depending on the research question, one could either include additional information about the temporal muscles, e.g., by measuring curve semilandmarks along the temporal lines, or "avoid" the crests completely, e.g., by distributing the semilandmarks on the internal table of the braincase (i.e. the surface of the endocast).

Placing semilandmarks

The requirement for homology must guide any landmark and semilandmark measurement protocol. Points that are well defined by the local anatomy in all directions should be treated as traditional landmarks. Clearly observable curves on surfaces, such as ridges, should be treated as curve semilandmarks rather than surface semilandmarks. The number of semilandmarks depends on the complexity of the curve or surface and on the spatial scale of shape variation that is of interest. For many applications the semilandmarks shown in Fig. 1–8 are probably more densely spaced than necessary. However, this redundant oversampling

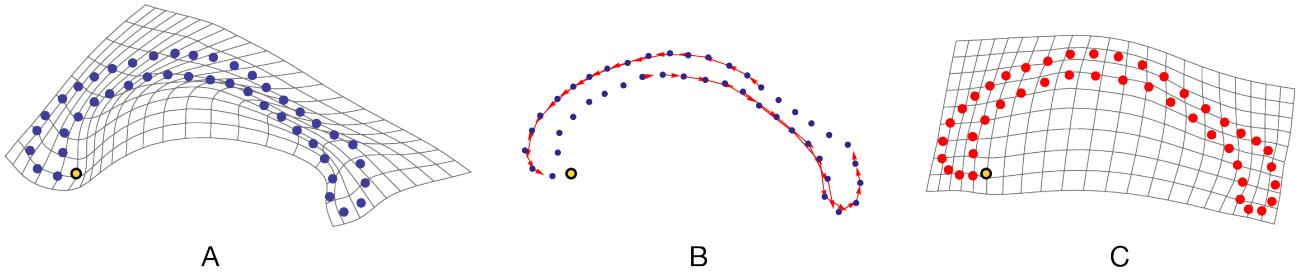

Figure 2 – One landmark (yellow) , and 87 curve semilandmarks were measured on the midline of the corpus callosum (see main text for details). TPS transformation grids between the Procrustes mean shape shape and one specimen before (A) and after semilandmark sliding (C). B: The initially equidistant curve semilandmarks (blue) slide (red arrows) along the curve until the TPS bending energy between this specimen and the Procrustes mean shape is minimal. Note that semilandmark sliding does not change the shape of the digitized curve, only the spacing of the semilandmarks along the curve changes.

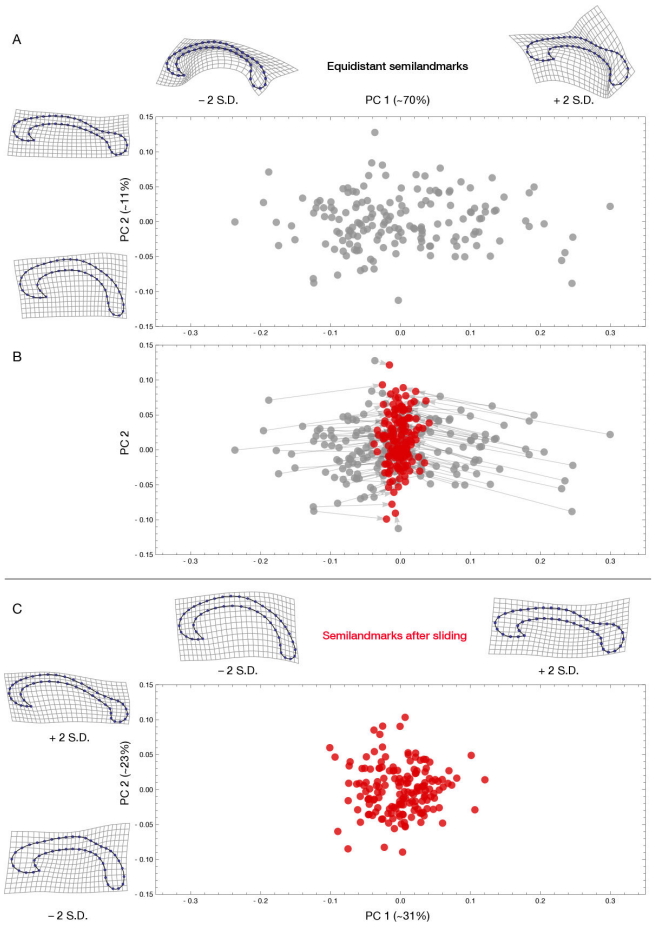

Figure 3 – Principal component (PC) scores of Procrustes shape coordinates before (A,B) and after semilandmark sliding (C). TPS transformation grids visualize the shape changes associated with the PC axes. B: the slid specimens (red) are projected into the PC space of the unslid (equidistant) specimens (gray). The first principal component of the equidistant semilandmarks is dominated by the effects of the semilandmark spacing (A).

of morphology is critical for effective visualizations and exploratory studies, as well as for estimating missing data (Mitteroecker and Gunz, 2009; Gunz et al., 2009b). In principle, it is always advantageous to capture the morphology in great detail using densely spaced semilandmarks. The only caveat is that the number of variables often exceeds the number of cases whereas many classical multivariate methods require an excess of cases over variables. It may thus be necessary to use dimension reduction techniques, such as principal component analysis, prior to other multivariate methods, or to use methods that impose no constraints on the number of variables, such as partial least squares analysis (Rohlf and Corti, 2000; Bookstein et al., 2003; Mitteroecker and Bookstein, 2007, 2008), between-group PCA (Mitteroecker and Bookstein, 2011), and permutation tests (Good, 2000); examples can be found in Mitteroecker et al. (2005) and Mitteroecker and Gunz (2009).

For curves in two or three dimensions, one usually starts by distributing a sequence of the same number of equidistantly spaced points along the curve. It is convenient (however, not algebraically necessary) to have the start and end of each curve delineated by real landmarks. While these roughly equidistant points can be placed manually, it is often practical to resample the curves to the same point count automatically.

Placing the same number of semilandmarks on homologous locations is more challenging for surfaces than it is for curves. One approach is to measure a mesh of surface semilandmarks on a single template specimen, and project this mesh onto all other forms in the sample: we start by measuring landmarks and curves on all specimens and automatically resample the curves to the same point count of equidistant curve semilandmarks. We then measure a mesh of surface semilandmarks on a template specimen and use the TPS interpolation function computed from the landmarks and curve semilandmarks to warp this mesh from the template to each specimen. These warped mesh points usually "float" in the vicinity of the actual surface of the specimen and therefore need to be lofted onto the surface before they can be used as surface semilandmarks. At this stage all specimens in a sample have the same number of landmarks, curve semilandmarks, and surface semilandmarks in approximately homologous positions.

Semilandmark sliding

In several geometric morphometric approaches to outline analysis, equidistant points along curves are analysed directly, however we will show below that equidistance can lead to serious statistical and visualisation artifacts. It is important to keep in mind that equidistance is an intuitive, yet arbitrary way of distributing semilandmarks, which does not necessarily lead to geometric or biological correspondence of the points across specimens (Bookstein, 1997; Gunz et al., 2005). Likewise, the spacing of surface semilandmarks is also arbitrary. The semilandmarks are thus allowed to slide along their curve or surface in order to remove the effects of the arbitrary spacing by "optimizing" the position of the semilandmarks with respect to the average shape of the entire sample (average of the Procrustes shape coordinates). The sliding algorithm is iterative: First the semilandmarks of each specimen are allowed to slide with respect to one (arbitrary) template specimen. Then one computes a Procrustes superimposition from these sled coordinates and a mean shape. Subsequently all semilandmarks are allowed to slide with respect to the average Procrustes shape.

Fig. 2 and 3 illustrate that equidistant semilandmarks can cause serious statistical and visualization artefacts. The semilandmarks were measured on magnetic resonance imaging (MRI) scans of human brains; they trace the midline of the corpus callosum, the structure in the brain that connects the two hemispheres. On 163 MRI scans we extracted the midsagittal slice, digitized one anatomical landmark, and distributed 87 equidistant curve-semilandmarks along the outline of the corpus callosum. We then allowed the equidistant semilandmarks on each individual to slide along the curve to minimize the TPS bending energy between this individual and the Procrustes mean shape. Fig. 2 shows the TPS transformation grid between the mean shape and one individual before (Fig. 2A) and after sliding (Fig. 2C). It is evident from Fig. 2 that semilandmark sliding has a profound effect on the TPS visualization: what looks like a strong local shape signal in the posterior part of the corpus callosum in Fig. 2A, turns out to be an artefact of the equidistant semilandmark spacing: this signal disappears when the semilandmarks are allowed to slide along the curve. We then computed two principal component analyses (PCA) in shape space to visualize the axes of largest shape variation. A comparison of the first two PC scores in shape space before (Fig. 3A) and after semilandmark sliding (Fig. 3B and 3C) reveals that the arbitrary semilandmark spacing accounts for the axis of largest variance in the dataset, the first principal component in shape space. In Fig. 3B the PC scores after semilandmark sliding (red) are projected into the PC space of the equidistant semilandmarks. This figure demonstrates that the shape variation along the first PC "disappears" almost completely when the semilandmarks are allowed to slide along the corpus callosum outline. As expected, the TPS transformation grids that visualize the shape changes along the first two principal components of shape space of the sled semilandmarks (Fig. 3C) are much smoother than the TPS transformation grids of Fig. 3A.

To make the computation of the semilandmark sliding computationally tractable, the semilandmarks slide on tangent lines to the respective curve, or on tangent planes to the respective surface (Fig. 4A). For curve semilandmarks these tangents are computed based on the two adjacent landmarks and semilandmarks; it is therefore convenient to start and end each curve with real landmarks, so reliable tangents can be computed for the first and last semilandmark along a curve. For surface semilandmarks the tangent planes are computed as the first two eigenvectors of the covariance matrix of adjacent points on the surface; for each semilandmark here we used the five closest landmarks

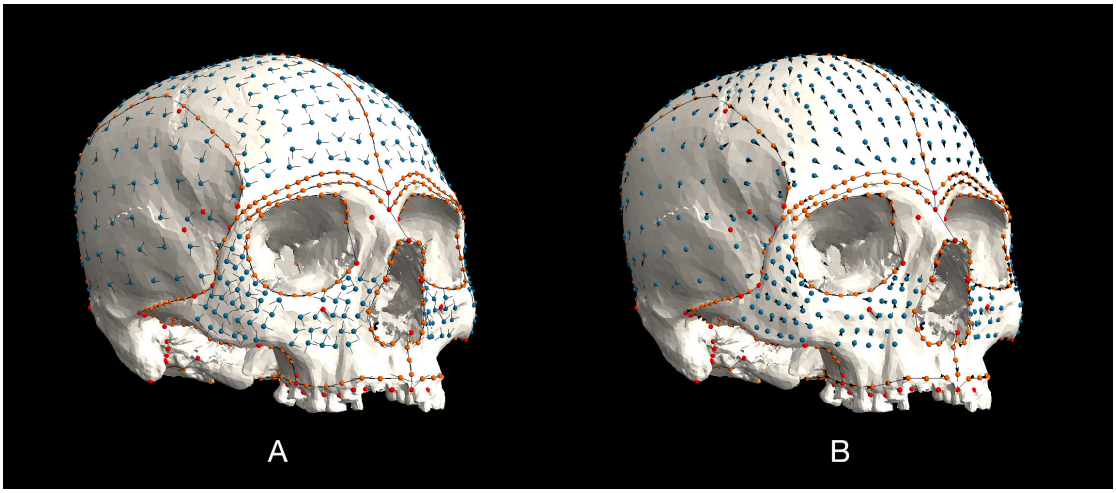

Figure 4 – Landmarks (red), curve semilandmarks (orange), and surface semilandmarks (blue) on a modern human cranium. A: Semilandmarks are allowed to slide along tangents (curves), and tangent planes (surfaces) so as to minimize the thin-plate spline bending energy between this specimen and the Procrustes average shape of the sample. B: After sliding, the semilandmarks are projected back onto the surface. Arrows connect semilandmarks before and after sliding. In this example, the positions of the semilandmarks change only subtly.

and semilandmarks to approximate the respective tangent planes. After each sliding step the slid semilandmarks can be projected back onto the curves or surfaces to ensure that they stay on the form. Whether or not this projection step is necessary depends on the complexity of the curve, the number of semilandmarks, and the amount of sliding. Fig. 4A shows the tangents for each curve semilandmark (orange spheres), and the two tangent vectors for each surface semilandmark (blue spheres). Fig. 4B visualizes the semilandmarks before and after sliding (minimizing bending energy) in a sample of *Homo sapiens* crania; it is evident that in this example the position of the semilandmarks only changes subtly.

Procrustes sliding *vs.* bending energy sliding

As mentioned above, there are two alternative computational approaches to sliding semilandmarks. In both approaches the semilandmarks slide so as to minimize shape differences between each specimen and the average shape in the sample. That is, shape variation due only to the arbitrary spacing of semilandmarks is reduced. The two approaches differ in the way shape differences are quantified, and so, in what is being minimized. In the most common approach, the one originally published by Bookstein (1997) and Gunz et al. (2005), the bending energy between all specimens and the average shape is minimized by the iterative sliding. Alternatively, it has been suggested to minimize Procrustes distance instead of bending energy (Fig. 5).

Minimizing bending energy is the optimal solution for producing transformation grids between specimens because both techniques are based on the TPS formalism. Bending energy only takes into account local shape deformation; uniform shape differences such as stretching and shearing have no effect on bending energy and the sliding process. Minimizing Procrustes distance, which is faster to compute than minimizing bending energy, is a least-squares procedure and more closely resembles the usual sum-of-squares decomposition in statistics. The most important difference, however, is the notion of homology implicit in the two approaches. Bending energy is based on all landmarks and semilandmarks and the "smoothness" of the shape deformation as a whole. All semilandmarks slide together and are influenced by the anatomical landmarks. When minimizing Procrustes distance, by contrast, each semilandmark slides separately and, apart from the common Procrustes superimposition, the sliding is not influenced by the other landmarks and semilandmarks. For instance, when minimizing Pro-

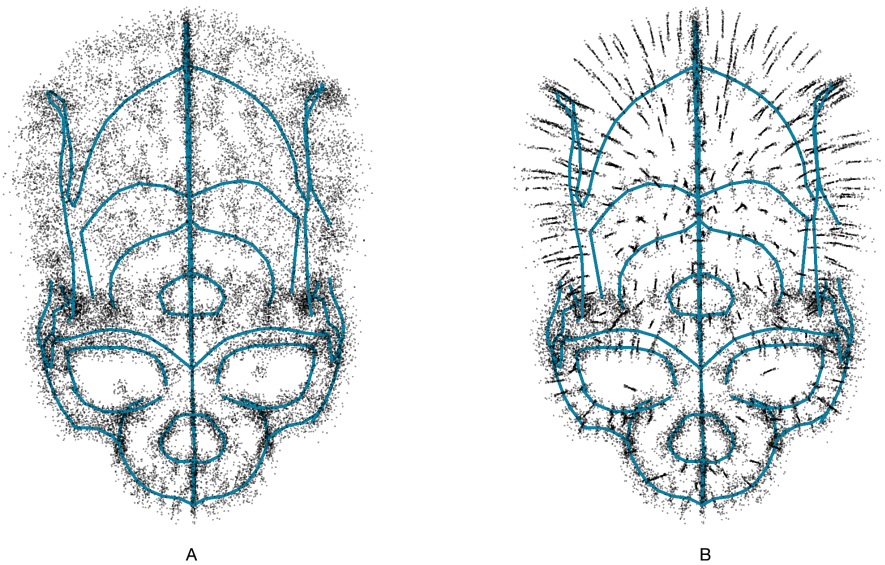

Figure 5 – Procrustes superimposition of 46 modern human crania. A: Semilandmarks were allowed to slide so as to minimize thin-plate spline bending energy between each specimen and the Procrustes average shape (blue curves). B: Semilandmarks were allowed to slide so as to mimize the Procrustes distance between each specimen and the Procrustes average shape.

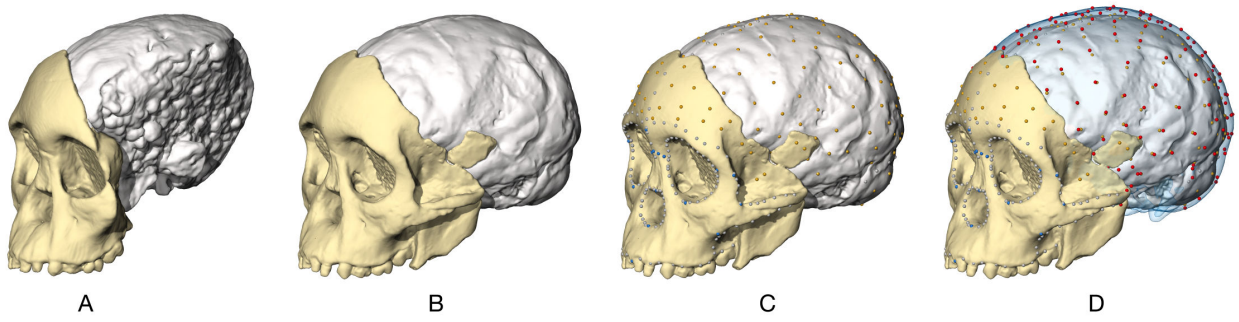

Figure 6 – Virtual reconstruction of the *Australopithecus africanus* fossil cranium Taung 1. A: Computed tomographic scan of the original fossil. B: Face and natural endocast were mirror-imaged on the computer. C: Landmarks (blue), curve semilandmarks (gray), surface semilandmarks (orange) were measured on the mirror-imaged version of the Taung child and a complete reference specimen (a subadult human). D: Landmarks and semilandmarks missing on the Taung child (red) were declared missing and estimated by allowing them to move freely so as to minimize the bending energy between Taung and the reference cranium. TPS interpolation was then used to warp the braincase of the human reference cranium to Taung (semitransparent blue surface).

crustes distance, curve semilandmarks can potentially slide beyond the endpoint of the curve or may pass another semilandmark. In contrast, this is almost impossible when minimizing bending energy. Both sliding approaches yield similar results if shape variation is small and if the semilandmarks do not need to slide much; for larger shape variation and more extensive sliding, minimizing bending energy usually leads to better results that are in line with our notion of biological homology. As mentioned above, a potential pathology is that semilandmarks end up on a different structure after sliding, e.g., semilandmarks on the frontal bone might "cross" the coronal suture and end up on the parietal bone. This is easily avoided when sliding minimizes bending energy, however, by placing a few real landmarks or curve landmarks on the coronal suture; these points will constrain the movement of the surface semilandmarks. Whether such constraints on sliding are desirable depends on the research question: for a comparison of overall braincase shape across genera the relative position of sutures might be not be particularly informative. In this case one might consider allowing semilandmarks to slide across the entire neurocranial surface, thereby ignoring sutures (Gunz et al., 2005). Incorporating landmarks or curve semilandmarks along sutures, in contrast, will be informative about individual development instead (i.e., how a particular neurocranium manages to realize its shape ontogenetically.)

Semilandmarks for missing data estimation

As GM methods require all specimens to have the same number of landmark and semilandmark coordinates, partially preserved specimens present a big challenge for any GM analysis. One can either restrict the analysis to the subset of landmarks and semilandmarks available on all specimens, or estimate the missing data. In many applications the first option is impractical, as the number of landmarks available on all specimens is often very small. In bilaterally symmetrical structures, like the skull, it usually best to start by mirror-imaging preserved parts from one side to the other (Gunz et al., 2009a, 2011, 2012; Weber and Bookstein, 2011; Weber et al., 2012; Neubauer et al., 2012; Benazzi et al., 2009; Benazzi and Senck, 2010; Benazzi et al., 2011a,b; Zollikofer et al., 1995, 1998; Ponce de León and Zollikofer, 1999, 2001; Zollikofer, 2002; Zollikofer et al., 2005; Ponce de León et al., 2008; Kalvin et al., 1995; O'Higgins et al., 2011; Zollikofer and Ponce de León, 2005). For parts that are missing on both sides, or in the symmetry axis, one can use the semilandmark algorithm to estimate the location of landmarks and semilandmarks that cannot be measured in a specimen, because, e.g., a part is broken off. At its core the concept of semilandmark sliding is already a missing data algorithm (Gunz et al., 2009a): the position of semilandmarks along a curve or surface is not well-defined and therefore not interesting; only their position in the direction normal to the curve or surface is relevant for the statistical analysis. In other words, a semilandmark's position along the curve or surface is missing: a curve semilandmark is missing one coordinate (along the tangent direction); a surface semilandmark is missing two (along the tangent plane); missing landmarks or semilandmarks are missing all three coordinates.

To estimate missing coordinates in an incomplete target form, a thin-plate spline interpolation is computed based on the landmarks and semilandmarks that are available in both a complete reference specimen and the incomplete target specimen. This interpolation function is used to map the missing landmarks and semilandmarks from the reference onto the target (Gunz et al., 2009b). This is accomplished during the sliding step, as missing landmarks and semilandmarks are allowed to move freely so as to minimize the bending energy between the incomplete specimen and a complete reference specimen.

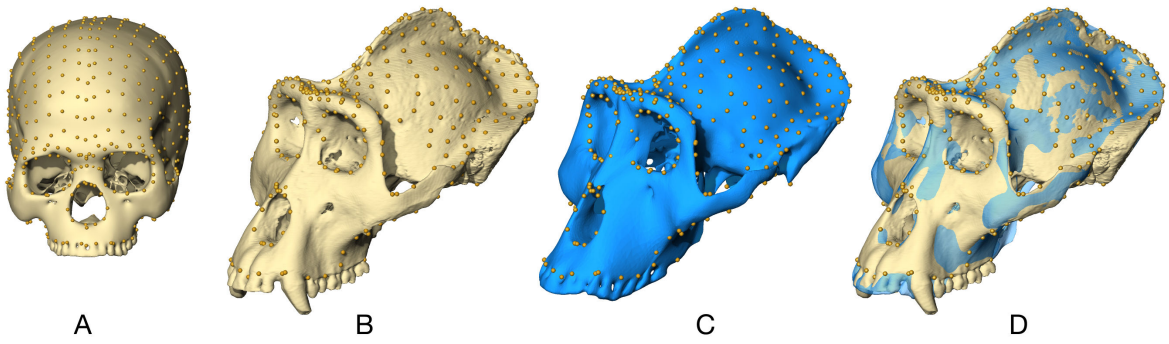

Figure 7 – Landmarks and semilandmarks on a modern human (A) and a gorilla male (B), were used to warp the modern human surface (C). D: Despite the substantial shape differences, the warped human surface (semitransparent blue) matches closely with the actual surface of the gorilla (bone colour).

We illustrate this virtual reconstruction protocol in Fig. 6, using a computed tomographic scan of a hominin fossil belonging to the species *Australopithecus africanus*. The holotype of this species, the subadult specimen Taung 1, comprises parts of the face, mandible, and a fossilized imprint of the braincase – a so-called natural endocast (Fig. 6A). After mirror-imaging across the midsagittal plane (Fig. 6B), we measured landmarks and semilandmarks on this specimen (Fig. 6C) and a complete reference cranium (a modern human subadult). We then used the TPS interpolation function to estimate the missing landmarks and semilandmarks on the exterior of the braincase in the child (Fig. 6D).

The accuracy of a virtual reconstruction depends upon the size of the defect and the number of coordinates that are recorded in the vicinity of the missing part such that reconstruction of a small defect with many adjacent coordinates will have greater accuracy (Gunz et al., 2009a; Grine et al., 2010; Weber at al., 2012; Benazzi et al., 2011a; Weber and Bookstein, 2011; Neubauer et al., 2012). A TPS interpolation can only be computed between two forms. As one might expect, the choice of the reference specimen used for estimation of the missing data will influence the final shape of the reconstruction. In most practical applications, however, it is impossible to determine what the "correct" reference form is. In Gunz et al. (2009b) we have therefore suggested creating multiple reconstructions based on as many reference forms as possible to assess the influence of the arbitrary reference choice. Shape differences among the resulting reconstructions of the same specimen provide a sense of the reconstruction uncertainty (Gunz et al., 2009a, 2010; Grine et al., 2010; Benazzi et al., 2011a; Neubauer et al., 2012; Gunz et al., 2012).

Applications and limitations

Using several hundred semilandmarks one can use a TPS interpolation to morph a human cranium into a gibbon (Fig. 1), and a gorilla (Fig. 7C). The surface warps are only used as visual aids here; however, the close correspondence between the actual gorilla surface and the warped human surface (Fig. 7D) confirms that after semilandmark sliding these point coordinates can be treated as homologous, even when the shape differences are fairly substantial, and even if there are few anatomical landmarks (like, e.g., on the neurocranium).

Applications of semilandmarks are not restricted to crania (Weber et al., 2001; Mitteroecker et al., 2004; Schaefer et al., 2004; Mitteroecker et al., 2004; Mitteroecker and Bookstein, 2008; Gunz et al., 2009a; Gonzalez et al., 2010; Heuzé et al., 2010; Benazzi et al., 2011a; Stansfield Nee Bulygina and Gunz, 2011; Weber and Bookstein, 2011; Weber at al., 2012), endocasts (Neubauer et al., 2004, 2005; Neubaer et al., 2009; Gunz et al., 2010; Neubauer et al., 2010, 2012; Gunz et al., 2012), or mandibles (Coquerelle et al., 2011; Benazzi et al., 2011b). They can also be used to quantify the enamel dentine junction (Skinner et al., 2008, 2009a; Skinner and Gunz, 2010) from high-resolution computed tomographic data of teeth (Fig. 8A), and the bony labyrinth of the inner ear (Fig. 8B). As shape is captured in such great detail using semilandmarks, it was possible to document subtle, yet statistically significant shape differences between subspecies of chimpanzees (*Pan troglodytes troglodytes* and *P. t. verus*), both for the enamel-dentine junction (Skinner et al., 2009a), and the semicircular canals of the inner ear (Gunz et al., 2012). The ability to discriminate dental shape and labyrinth shape at the subspecies level demonstrates that semilandmarks can be extremely useful in taxonomic studies of extant and fossil specimens (Gunz et al., 2012). It is not only possible to capture very subtle shape differences among groups, one can also visualize the results of the statistical analysis as shape deformations.

Semilandmarks (like all geometric morphometric techniques) are not suitable for the comparison of forms when the curves and surfaces are not homologous among specimens. The method was also developed for capturing fairly smooth surfaces and sharp ridges, so there are practical limitations regarding the complexity of surfaces. While it is, e.g., possible to quantify the relatively smooth surface of brain endocasts using semilandmarks (Neubaer et al., 2009), the gyri and sulci of the brain's surface might prove to be too complex and irregular for semilandmarks.

Semilandmarks and alternative methods

Several alternative morphometric approaches exist for quantifying curves and surfaces. Of particular interest are recent methodological advances that require less manual input than the sliding semilandmark approach discussed here. In these "homology-free" methods (for reviews see Polly 2008; Klingenberg 2008) the forms usually are aligned first – either based on a few landmarks, or completely automatically based on principal axes; subsequently a correspondence map between two shapes is computed automatically (Specht et al., 2007; Polly, 2008; Durrelman et al., 2011; Boyer et al., 2011). The obvious advantage of such a semi-automated data collection is the possibility to process large sample sizes in a fairly short amount of time (Polly, 2008; Klingenberg, 2008). The processing speed comes at a cost, however. Many automated methods are restricted to fairly small ranges of shape variation. Moreover, the point homology across specimens, which is "enforced" by the experienced morphometrician measuring semilandmarks on curves and surfaces manually, is no longer guaranteed. As a result, sample averages and variances may be meaningless and biologically not interpretable. If one aims to go beyond the mere discrimination of groups and tries to identify the biological factors underlying shape differences, the time spent digitizing curves and surfaces as semilandmarks is almost always worthwhile.

Software tools

Sliding semilandmarks for two-dimensional data (usually digitized from images) can easily be handled by the free TPS series by Jim Rohlf (http://life.bio.sunysb.edu/ee/rohlf/software.html). Three-dimensional

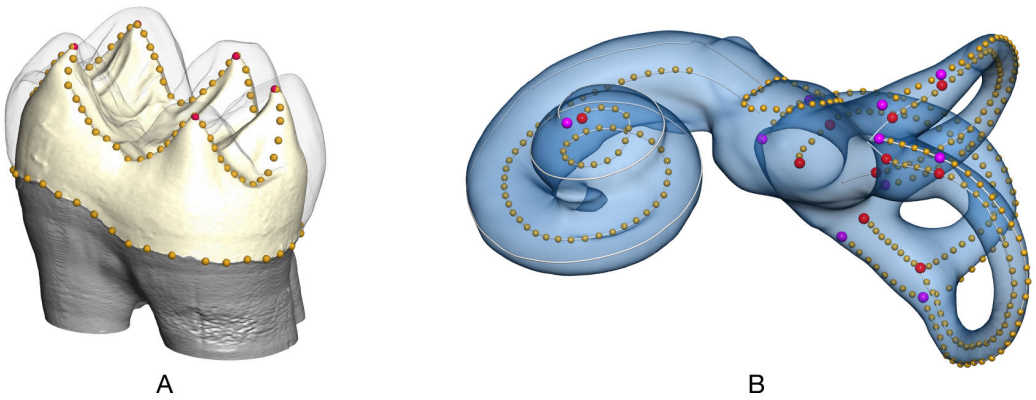

Figure 8 – A: Landmarks (red) and curve semilandmarks (orange) quantify the enamel-dentine junction of a molar based on a micro CT scan (Skinner et al., 2008, 2009a,b; Skinner and Gunz, 2010). B: Landmarks (red and magenta) and curve semilandmarks (orange) on the bony labyrinth of the inner ear (Gunz et al., 2012).

semilandmarks are supported by the EVAN toolbox by the EVAN Society (http://evan-society.org/), and the commercial software package Viewbox (http://www.dhal.com/). Scripts for sliding semilandmarks in the statistical software package R (http://www.R-project.org), developed by Stefan Schlager are available (http://sourceforge.net/projects/morpho-rpackage). The Mathematica (Wolfram Inc.) code for 2D and 3D sliding semilandmarks developed by the authors, which was used to create the figures and analyses in this paper, is available from the authors upon request.

References

Adams D.C., Rohlf F.J., Slice D.E., 2004. Geometric morphometrics: ten years of progress following the "revolution". Italian Journal of Zoology 71: 5–16.

Benazzi S., Bookstein F.L., Strait D.S., Weber G.W., 2011. A new OH5 reconstruction with an assessment of its uncertainty. J. Hum. Evol. 61(1): 75–88.

Benazzi S., Fiorenza L., Kozakowski S., Kullmer O., 2011. Comparing 3D Virtual Methods for Hemimandibular Body Reconstruction. Anat. Rec. (Hoboken) 294(7): 1116–1125.

Benazzi S., Senck S., 2010. Comparing 3-Dimensional Virtual Methods for Reconstruction in Craniomaxillofacial Surgery. J. Oral. Maxillofac. Surg. 69(4): 1184–1194.

Benazzi S., Stansfield E., Milani C., Gruppioni G., 2009. Geometric morphometric methods for three-dimensional virtual reconstruction of a fragmented cranium: the case of Angelo Poliziano. Int. J. Legal. Med. 123: 333–344.

Bookstein F.L., 1989. Principal warps: Thin-plate splines and the decomposition of deformations. IEEE. Transactions on Pattern Analysis and Machine Intelligence V: 567–585.

Bookstein F.L., 1991. Morphometric Tools for Landmark Data: Geometry and Biology. Cambridge University Press, Cambridge, UK.

Bookstein F.L., 1994. Can biometrical shape be a homologous character? In: Hall B.K. (Ed.). Homology: The Hierarchical Basis of Comparative Biology. Academic Press, New York. 197–227.

Bookstein F.L., 1997. Landmark methods for forms without landmarks: morphometrics of group differences in outline shape. Med. Image. Anal. 1: 225–243.

Bookstein F.L., Gunz P., Mitteroecker P., Prossinger H., Schaefer K., Seidler H., 2003. Cranial integration in *Homo*: singular warps analysis of the midsagittal plane in ontogeny and evolution. J. Hum. Evol. 44: 167–187.

Boyer D.M., Lipman Y., St. Clair E., Puente J., Patel B.A., Funkhouser T., Jernvall J., Daubechies I., 2011. Algorithms to automatically quantify the geometric similarity of anatomical surfaces. Proc. Natl. Acad. Sci. U.S.A. 108: 18221–18226.

Coquerelle M., Bookstein F.L., Braga J., Halazonetis D.J., Weber G.W., Mitteroecker P., 2011. Sexual dimorphism of the human mandible and its association with dental development. Am. J. Phys. Anthropol. 145: 192–202.

Dryden I.L., Mardia K.V., 1998. Statistical Shape Analysis. John Wiley & Sons, London, Chichester.

Durrleman S., Pennec X., Trouvé A., Ayache N., Braga J., 2011. Comparison of the endocranial ontogenies between chimpanzees and bonobos via temporal regression and spatiotemporal registration. J. Hum. Evol. 62(1): 74–88.

Gonzalez P.N., Perez S.I., Bernal V., 2010. Ontogeny of robusticity of craniofacial traits in modern humans: a study of South American populations. Am. J. Phys. Anthropol. 142: 367–379.

Good P.I., 2000. Permutation tests: a practical guide to resampling methods for testing hypotheses. Springer, New York.

Grine F.E., Gunz P., Betti-Nash L., Neubauer S., Morris A.G., 2010. Reconstruction of the Late Pleistocene human skull from Hofmeyr, South Africa. J. Hum. Evol. 59: 1–15.

Gunz P., Bookstein F.L., Mitteroecker P., Stadlmayr A., Seidler H., Weber G.W., 2009. Early modern human diversity suggests subdivided population structure and a complex out-of-Africa scenario. Proc. Natl. Acad. Sci. U.S.A. 106: 6094-6098.

Gunz P., Mitteroecker P., Bookstein F.L., 2005. Semilandmarks in three dimensions. In: Slice D.E. (Ed.). Modern Morphometrics in Physical Anthropology. Kluwer Academic/Plenum Publishers, New York. 73–98.

Gunz P., Mitteroecker P., Neubauer S., Weber G.W., Bookstein F.L., 2009. Principles for the virtual reconstruction of hominin crania. J. Hum. Evol. 57: 48–62.

Gunz P., Neubauer S., Golovanova L., Doronichev V., Maureille B., Hublin J.J., 2012. A uniquely modern human pattern of endocranial development. Insights from a new cranial reconstruction of the Neandertal newborn from Mezmaiskaya. J. Hum. Evol. 62: 300–313.

Gunz P., Neubauer S., Maureille B., Hublin J.J., 2010. Brain development after birth differs between Neanderthals and modern humans. Current Biology 20: R921-R922.

Gunz P., Neubauer S., Maureille B., Hublin J.J., 2011. Virtual Reconstruction of the Le Moustier 2 newborn skull. Implications for Neandertal ontogeny. PALEO 22: 155–172.

Gunz P., Ramsier M., Kuhrig M., Hublin J.J., Spoor F., 2012. The mammalian bony labyrinth reconsidered, introducing a comprehensive geometric morphometric approach. J. Anat. 220(6): 529–543.

Hall B.K., 2003. Descent with modification: the unity underlying homology and homoplasy as seen through an analysis of development and evolution. Biological Reviews 78: 409-433.

Heuzé Y., Boyadjiev S.A., Marsh J.L., Kane A.A., Cherkez E., Boggan J.E., Richtsmeier J.T., 2010. New insights into the relationship between suture closure and craniofacial dysmorphology in sagittal nonsyndromic craniosynostosis. J. Anat. 217: 85–96.

Kalvin A.D., Dean D., Hublin J.-J., 1995. Reconstruction of human fossils. IEEE Computer Graphics and. Applications 15: 12–15.

Kendall D.G., 1984. Shape manifolds, Procrustean metrics and complex projective spaces. Bull. London Math. Soc. 16: 81–121.

Klingenberg C.P., 2008. Novelty and "Homology-free´´ Morphometrics: What's in a Name? Evolutionary Biology 35: 186–190.

Mitteroecker P., Bookstein F., 2007. The conceptual and statistical relationship between modularity and morphological integration. Syst. Biol. 56: 818–836.

Mitteroecker P., Bookstein F., 2008. The evolutionary role of modularity and integration in the hominoid cranium. Evolution 62: 943–958.

Mitteroecker P., Bookstein F., 2011. Linear Discrimination, Ordination, and the Visualization of Selection Gradients in Modern Morphometrics. Evolutionary Biology 39: 100–114.

Mitteroecker P., Gunz P., 2009. Advances in Geometric Morphometrics. Evolutionary Biology 36: 235–247.

Mitteroecker P., Gunz P., Bernhard M., Schaefer K., Bookstein F.L., 2004. Comparison of cranial ontogenetic trajectories among great apes and humans. J. Hum. Evol. 46: 679–697.

Mitteroecker P., Gunz P., Bookstein F.L., 2005. Heterochrony and geometric morphometrics: A comparison of cranial growth in *Pan paniscus* versus *Pan troglodytes*. Evolution and Development 7: 244–258.

Mitteroecker P., Gunz P., Weber G.W., Bookstein F.L., 2004. Regional dissociated heterochrony in multivariate analysis. Annals of Anatomy 186: 463–470.

Neubauer S., Gunz P., Hublin J.J., 2009. The pattern of endocranial ontogenetic shape changes in humans. J. Anat. 215: 240–255.

Neubauer S., Gunz P., Hublin J.J., 2010. Endocranial shape changes during growth in chimpanzees and humans: a morphometric analysis of unique and shared aspects. J. Hum. Evol. 59: 555–566.

Neubauer S., Gunz P., Mitteroecker P., Weber G.W., 2004. Three-dimensional digital imaging of the partial *Australopithecus africanus* endocranium MLD 37/38. Can. Assoc. Radiol. J. 55: 271–278.

Neubauer S., Gunz P., Schwarz U., Hublin J.J., Boesch C., 2012. Endocranial Volumes in an Ontogenetic Sample of Chimpanzees from the Tai Forest National Park, Ivory Coast. Am. J. Phys. Anthropol. 147(2): 319–325. doi:10.1002/ajpa.21641

Neubauer S., Gunz P., Weber G.W., 2005. Digital reconstruction of *P. boisei* OH 5. Am. J. Phys. Anthropol. Suppl. 40: 161.

Neubauer S., Gunz P., Weber G.W., Hublin J.J., 2012. Endocranial volume of *Australopithecus africanus*: New CT-based estimates and the effects of missing data and small sample size. J. Hum. Evol. 62(4): 498–510.

O'Higgins P., Cobb S.N., Fitton L.C., Gröning F., Phillips R., Liu J., Fagan M.J., 2011. Combining geometric morphometrics and functional simulation: an emerging toolkit for virtual functional analyses. J. Anat. 218: 3–15.

Oxnard C., O'Higgins P., 2009. Biology Clearly Needs Morphometrics. Does Morphometrics Need Biology? Biological Theory 4: 84–89.

Perez S.I., Bernal V., Gonzalez P.N., 2006. Differences between sliding semi-landmark methods in geometric morphometrics, with an application to human craniofacial and dental variation. J. Anat. 208: 769–784.

Polly P.D., 2008. Developmental Dynamics and G-Matrices: Can Morphometric Spaces be Used to Model Phenotypic Evolution? Evolutionary Biology 35: 83–96.

Ponce de León M.S., Golovanova L., Doronichev V., Romanova G., Akazawa T., Kondo O., Ishida H., Zollikofer C.P., 2008. Neanderthal brain size at birth provides insights into the evolution of human life history. Proc. Natl. Acad. Sci. U.S.A. 105: 13764–13768.

Ponce de León M.S., Zollikofer C.P., 1999. New evidence from Le Moustier 1: computer-assisted reconstruction and morphometry of the skull. Anat. Rec. 254: 474–489.

Ponce de León M.S., Zollikofer C.P., 2001. Neanderthal cranial ontogeny and its implications for late hominid diversity. Nature 412: 534–538.

Rohlf F.J., Corti M., 2000. Use of two-block partial least-squares to study covariation in shape. Syst. Biol. 49: 740–753.

Rohlf F.J., Slice D., 1990. Extensions of the Procrustes method for the optimal superimposition of landmarks. Syst. Zool. 39: 40–59.

Schaefer K., Mitteroecker P., Gunz P., Bernhard M., Bookstein F.L., 2004. Craniofacial sexual dimorphism patterns and allometry among extant hominids. Annals of Anatomy 186: 471–478.

Skinner M.M., Gunz P., 2010. The presence of accessory cusps in chimpanzee lower molars is consistent with a patterning cascade model of development. J. Anat. 217(3): 245–253.

Skinner M.M., Gunz P., Wood B.A., Boesch C., Hublin J.J., 2009. Discrimination of extant *Pan* species and subspecies using the enamel-dentine junction morphology of lower molars. Am. J. Phys. Anthropol. 140: 234–243.

Skinner M.M., Gunz P., Wood B.A., Hublin J.J., 2008. Enamel-dentine junction (EDJ) morphology distinguishes the lower molars of *Australopithecus africanus* and *Paranthropus robustus*. J. Hum. Evol. 55: 979–988.

Skinner M.M., Gunz P., Wood B.A., Hublin J.J., 2009. How Many Landmarks? Assessing the Classification Accuracy of *Pan* Lower Molars Using a Geometric Morphometric Analysis of the Occlusal Basin as Seen at the Enamel-Dentine Junction. Front. Oral. Biol. 13: 23–29.

Slice D.E., 2007. Geometric morphometrics. Annu. Rev. Anthropol. 36: 261–281.

Specht M., Lebrun R., Zollikofer C.P.E., 2007. Visualizing shape transformation between chimpanzee and human braincases. Visual. Computer 23: 743–751.

Stansfield Nee Bulygina E., Gunz P., 2011. Skhodnya, Khvalynsk, Satanay, and Podkumok calvaria: possible Upper Paleolithic hominins from European Russia. J. Hum. Evol. 60: 129–144.

Thompson D., 1917. On Growth and Form. Cambridge University Press, Cambridge, UK.

Weber G.W., Bookstein F.L., 2011. Virtual anthropology: a guide to a new interdisciplinary field. Springer, Wien, London.

Weber G.W., Gunz P., Neubauer S., Mitteroecker P., Bookstein F.L., 2012. Digital South African fossils: morphological studies using reference-based reconstruction and electronic preparation. In: Reynolds S.C., Gallagher A. (Eds.). African Genesis: Perspectives on Hominin Evolution. Cambridge University Press, Cambridge, UK. 298–316.

Weber G.W., Schaefer K., Prossinger H., Gunz P., Mitteroecker P., Seidler H., 2001. Virtual anthropology: the digital evolution in anthropological sciences. J. Physiol. Anthropol. Appl. Human. Sci. 20: 69–80.

Zollikofer C.P., Ponce de León M.S., Lieberman D.E., Guy F., Pilbeam D., Likius A., Mackaye H.T., Vignaud P., Brunet M., 2005. Virtual cranial reconstruction of *Sahelanthropus tchadensis*. Nature 434: 755–759.

Zollikofer C.P.E., 2002. A Computational Approach to Paleoanthropology. Evolutionary Anthropology 11: 64-67.

Zollikofer C.P.E., Ponce de Leon M.S., Martin R.D., Stucki P. 1995. Neanderthal computer skulls. Nature. 375: 283–285.

Zollikofer C.P.E., Ponce de León M.S., 2005. Virtual reconstruction: a primer in computer-assisted paleontology and biomedicine. Wiley-Interscience, Hoboken, N.J.

Zollikofer C.P.E., Ponce De León M.S., Martin R.D., 1998. Computer-assisted paleoanthropology. Evolutionary Anthropology 6: 41–54.

Associate Editor: A. Loy